makes curvature harder to detect. If oxygen was consumed primarily from the oxygenated bottom water, then the oxygen could have been resupplied from the surroundings at a high rate. This would prevent any large curvature from appearing and oxygen would seem to behave conservatively. Oxygen uptake by the hydrothermal vent clam *Calyptogena* appears to occur at near ambient conditions, whereas sulfide is consumed in warmer water with higher sulfide concentrations (*19*).

There was 27 μM less sulfide and 37 μM less oxygen at location B than at location C at a silicate concentration of 400 μM. The extra sulfide and oxygen consumed at location B was removed in a ratio of 0.73 to 1. It is difficult to determine the oxidation product of sulfide from these results, however, because community oxygen demand will consume oxygen without sulfide. Anaerobic sulfide oxidation is also possible.

Our in situ measurements demonstrate large variability in sulfide and silicate concentrations in the vicinity of the animals of this hydrothermal vent community. Consumption of sulfide by the vent animals was also evident. Direct calculations of the community metabolism will be possible when measurements of flow rates around these animals become available.

REFERENCES AND NOTES

1. J. B. Corliss *et al.*, *Science* **203**, 1073 (1979).
2. RISE Project Group: F. N. Spiess *et al.*, *ibid.* **207**, 1421 (1980).
3. E. Suess and G. J. Massoth, *Trans. Am. Geophys. Union* **65**, 1089 (1984).
4. C. K. Paull *et al.*, *Science* **226**, 965 (1984).
5. J. M. Brooks, M. C. Kennicutt II, R. R. Bidigare, R. A. Fay, *Trans. Am. Geophys. Union* **66**, 106 (1985).
6. H. Felbeck, *Science* **213**, 336 (1981); J. J. Childress and T. J. Mickel, *Mar. Biol. Lett.* **3**, 73 (1982); J. J. Childress, A. J. Arp, C. R. Fisher, Jr., *Mar. Biol.* **83**, 109 (1984).
7. J. M. Edmond *et al.*, *Earth Planet. Sci. Lett.* **46**, 19 (1979).
8. J. A. Wehlan and H. Craig, *Geophys. Res. Lett.* **6**, 829 (1979).
9. G. H. Rau and J. I. Hedges, *Science* **203**, 648 (1979); G. H. Rau, *ibid.* **213**, 338 (1981).
10. The Rose Garden is located at a depth of 2460 m at 00°48.247′N, 86°13.478′W. See R. D. Ballard, T. H. van Andel, and R. T. Holcomb [*J. Geophys. Res.* **87**, 1149 (1982)] for a description of the Galápagos Rift at this location.
11. J. Ruzicka and E. H. Hansen, *Flow Injection Analysis* (Wiley-Interscience, New York, 1981).
12. Silicate was determined as the reduced silicomolybdate dye [J. Thomsen, K. S. Johnson, R. L. Petty, *Anal. Chem.* **55**, 2378 (1983)]. We analyzed sulfide with the methylene blue technique [J. D. Cline, *Limnol. Oceanogr.* **14**, 454 (1969)] after adapting the method to FIA. Reagents were introduced into the system with "T" fittings rather than injection valves to give a continuous response. There is a 4-minute lag period while the sample is transported to the detector at a flow rate of 2 ml/min. Step changes in the concentration at the inlet appear as exponential changes at the detector with a 90 percent rise time of 40 seconds due to smear in the flow system.
13. J. M. Edmond *et al.*, *Earth Planet. Sci. Lett.* **46**, 1 (1979).
14. N. A. Duke and R. W. Hutchinson, *Can. J. Earth Sci.* **11**, 53 (1974).
15. R. M. Haymon and M. Kastner, *Earth Planet. Sci. Lett.* **53**, 363 (1981).
16. The time needed for vent water to mix from a temperature of 8° to 2°C must be no more than a few minutes since a distance of less than 50 cm separates these temperatures [R. R. Hessler and W. M. Smithey, Jr., in *Hydrothermal Processes at Seafloor Spreading Centers*, P. A. Rona *et al.*, Eds. (Plenum, New York, 1983), pp. 735–770; (*1*); Fig. 1]. At least 10 μM of sulfide are oxidized in this time period at location C (Fig. 2). A conservative estimate of the oxidation rate is 1 μmol/liter per minute. The oxidation rate measured in the laboratory under similar conditions of temperature, salinity, and *p*H is 0.02 μmol/liter per minute [J. D. Cline and F. A. Richards, *Environ. Sci. Technol.* **3**, 838 (1969)].
17. H. Felbeck, J. J. Childress, G. N. Somero, *Nature (London)* **293**, 291 (1981).
18. K. L. Smith, Jr., *Ecology* **66**, 1067 (1985).
19. A. J. Arp, J. J. Childress, C. R. Fisher, Jr., *Physiol. Zool.* **57**, 648 (1984).
20. A. C. Harvey, *The Econometric Analysis of Time Series* (Wiley, New York, 1981).
21. A. Savitzky and M. J. E. Golay, *Anal. Chem.* **36**, 1627 (1964).
22. M. D. Lilley, J. A. Baross, L. I. Gordon, in *Hydrothermal Processes at Seafloor Spreading Centers*, P. A. Rona *et al.*, Eds. (Plenum, New York, 1983), pp. 411–449.

23. This work was supported by NSF grant OCE83-11256. Development of the Scanner was also supported by Office of Naval Research contract N00014-82-K-0740. We thank R. Haymon, S. Willason, R. Hessler, and K. Smith for constructive reviews of the manuscript. We also thank the officers, crew, and pilots of the *Alvin/Atlantis II* group for their generous assistance.

2 August 1985; accepted 13 December 1985

Endonucleolytic Activity That Cleaves Immunoglobulin Recombination Sequences

THOMAS J. HOPE, RENATO J. AGUILERA, MARK E. MINIE, HITOSHI SAKANO

An endonucleolytic activity has been identified in nuclear extracts of chick embryo bursa and mouse fetal liver cells. The activity introduces a double-strand cut in the vicinity of the recombination site of immunoglobulin joining gene segments. The cleavage occurs at the dinucleotide pair $\frac{TG}{AC}$. This activity is a good candidate for the putative endonuclease involved in recombination of the immunoglobulin variable, diversity, and joining regions. It is distinct from the endonuclease activities previously reported by others.

IMMUNOGLOBULIN (IG) VARIABLE REgion genes are generated by site-specific DNA recombinations during the differentiation of B lymphocytes (*1*). In the light chain genes, the recombination takes place between two DNA segments, V and J (*2–5*). In the heavy chain genes, an additional DNA segment D (diversity) is involved (*6–8*); thus, two recombination events, V-D and D-J joinings are necessary to generate a complete heavy chain gene.

Nucleotide sequence analysis of the germline DNA segments revealed that two consensus sequences, CACTGTG and GGTTTTTGT, are always found at the recombination site, and the spacer separating the two sequences is either 12 or 23 base pairs (bp) long (*3, 6–8*). DNA recombination takes place between two pairs of palindromic conserved sequences, with one pair being separated by a 12-bp spacer and the other by a 23-bp spacer (12–23 bp spacer rule) (*6, 7*).

In order to better understand the molecular mechanism of Ig gene recombination, we have attempted to identify a recombination enzyme which mediates V-(D)-J joining. Our studies are based on the assumption that three main activities should be involved in Ig gene recombination: a DNA binding activity, an endonucleolytic activity, and a ligase activity. The binding activity could bring the two recombination sites together into the proper orientation, satisfying the 12–23 bp spacer rule. The endonucleolytic activity is then required to cut or nick the germline DNA around the recombination site. Finally, the ligase activity must join the two Ig sequences covalently.

We first attempted to identify a specific endonucleolytic activity that cleaves Ig gene sequences at or near the recombination site (*9*). We used mouse fetal liver and chick embryo bursa as enzyme sources because B-cell progenitors are assumed to first appear in these tissues during embryonic development (*10, 11*). We prepared nuclear extracts from these tissues (*12*), and fractionated them by column chromatography. An endonucleolytic activity that cleaves in the Ig joining segment region was identified by a Southern blot hybridization assay. To ascertain where the joining region cleavage occurs we used a DNA sequencing gel system (*13*) to analyze the cleavage products with chemically cleaved DNA as a size marker. We now report that mouse fetal liver nuclei contain an endonucleolytic activity that cleaves mouse $J_{\lambda 1}$ (λ, lambda chain) DNA between the conserved heptamer and the $J_{\lambda 1}$ coding sequence.

Department of Microbiology and Immunology, University of California, Berkeley, CA 94720.

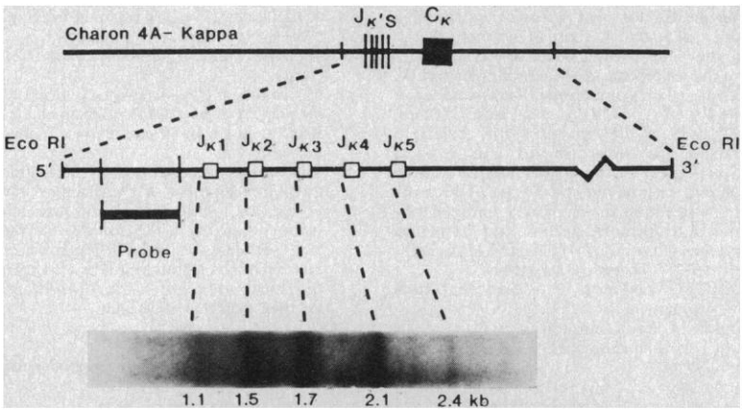

Fig. 1. In vitro cleavage of mouse J_{κ} DNA with mouse fetal liver nuclear extract detected by Southern hybridization (*14*). Phage DNA carrying a 16-kb Eco RI insert containing the mouse J_{κ} gene locus was incubated with DE52 fractionated nuclear extracts of 17- to 19-day-old mouse fetal liver. The reaction volume was 20 μl and contained 0.5 μg of J_{κ} phage DNA, 50 μg of sonicated salmon sperm DNA as a carrier, 2 μl 10× cleavage reaction buffer (100 m*M* Tris-Cl, *p*H 7.5, 100 m*M* MgCl, 60 m*M* DTT, 200 m*M* NaCl), and 5 μl of the DE52 flow through fraction of fetal liver nuclear extract. The reaction mixture was incubated for 30 minutes at 37°C. The reaction was stopped by heating at 65°C for 10 minutes. Denatured proteins were removed by centrifugation. The supernatant was then completely digested with Eco RI. The reacted DNA was then separated in an 0.8 percent agarose gel, transferred to a nitrocellulose filter and was hybridized with the Hind III 5′ J_{κ} probe. Southern hybridization with a 5′ J_{κ} probe revealed several discrete DNA fragments in which the cleavage sites correspond to the five J_{κ} genes. Nuclear extracts were prepared by a modification of the salt extraction of nuclei (*11*). Cells and homogenates were kept on ice throughout the procedure. Tissue was minced and washed twice in chilled buffer A (10 m*M* Hepes *p*H 7.9, 1.5 m*M* MgCl, 10 m*M* KCl, 0.5 m*M* DTT). Washed cells were centrifuged for 10 minutes at 750*g* at 4°C and resuspended in twice the original cell volume buffer A. Cells were disrupted in a Dounce homogenizer (ten strokes). The homogenate was centrifuged at 750*g* for 10 minutes at 4°C to separate the nuclei. Nuclei were resuspended in 2× cell volume buffer A and centrifuged at 25,000*g* for 20 minutes at 4°C, to remove cytoplasmic debris. Nuclei were resuspended in 2× original cell volume with salt extraction buffer (20 m*M* Hepes *p*H 7.9, 25 percent (by volume) glycerol, 420 m*M* NaCl, 0.5 m*M* DTT, 0.5 m*M* PMSF) with ten strokes of the Dounce tissue homogenizer. The resulting suspension was stirred with a magnetic bar for 30 minutes on ice and centrifuged at 25,000*g* for 30 minutes at 4°C. The clear supernatant was dialyzed against (20 m*M* Hepes *p*H 7.9, 20 percent (by volume) glycerol, 0.2 m*M* EDTA, 0.5 m*M* DTT/0.5 m*M* DMSF). The dialyzate was centrifuged at 25,000*g* for 20 minutes at 4°C. The resulting nuclear extract was separated into measured portions and frozen in liquid nitrogen and stored at −70°C where it is quite stable.

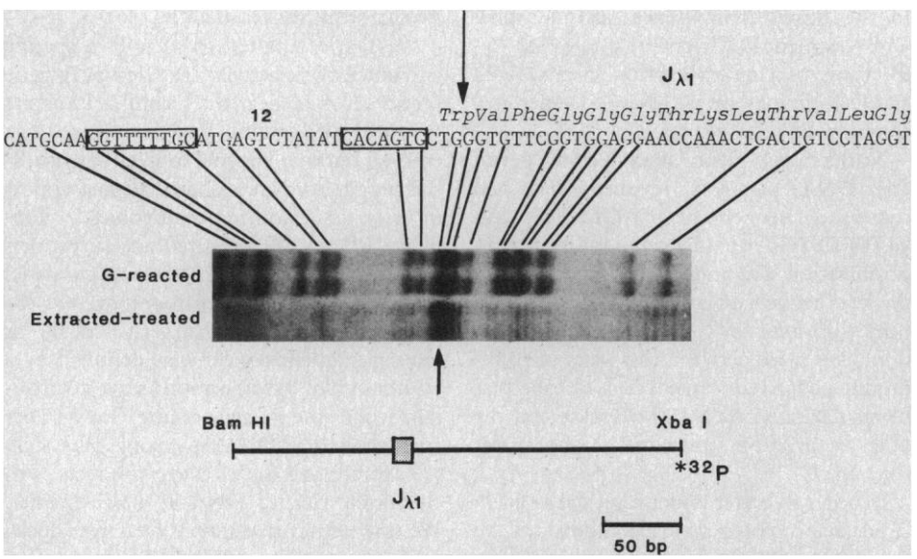

Fig. 2. In vitro cleavage of $J_{\lambda}1$ gene segment detected by sequencing gel assay. A 300-bp Bam HI–Xba I fragment was labeled at the Xba I end with ^{32}P. A cleavage is evident at the 5′ end of the $J_{\lambda}1$ coding region. The reaction mixture contained 1 μg of sonicated salmon sperm DNA, 1 μl of 10× cleavage reaction buffer, ^{32}P end-labeled $J_{\lambda}1$ DNA, and 5 μl of the DE52 flow through fraction of mouse fetal liver nuclear extract in a 10-μl volume. The mixture was incubated for 30 minutes at 37°C. The sample was then separated on a urea-containing 6 percent polyacrylamide gel along with a Maxam-Gilbert G reacted sample of the same end-labeled fragment as a size marker.

For the cleavage assay, J_{κ} (κ, kappa chain) containing DNA was used as a substrate in the initial experiments (Fig. 1). Phage DNA (charon 4A) containing the five J_{κ} gene segments (*3*) was incubated with fetal liver nuclear extract from 17- to 19-day-old mouse embryos. Nuclear extracts were prepared by the extraction of isolated fetal liver nuclei with 420 m*M* NaCl and subsequent dialysis (*12*). The reacted DNA was digested with Eco RI, and analyzed (*14*). If a specific cleavage took place at the recombination site of each J_{κ} gene segment, we would expect to detect a series of DNA fragments starting with the Eco RI site upstream of the J_{κ} region (Fig. 1). The cleavage products would be detected with a probe containing the 5′ J_{κ} sequence. The standard reaction mixture contained 5 μl of nuclear extract, 10 m*M* tris-Cl, *p*H 7.5, 10 m*M* MgCl, 20 m*M* NaCl, 1 m*M* EDTA, and 10 μg of sonicated salmon sperm DNA in a 20-μl reaction mixture. Since the extract contained a considerable amount of nonspecific nuclease activity, an excess amount of salmon sperm DNA was added to the reaction mixture, which was then incubated for 30 minutes at 37°C. The mouse fetal liver nuclear extracts were fractionated on DE52 (Whatman) to separate nonspecific nuclease activities. Several discrete bands were produced specifically with digestion by the DE52 flow-through fraction (Fig. 1). This suggested that a cleavage was taking place at each of the J_{κ} gene segments.

The exact location of the cleavage site was determined in a series of experiments with fetal liver extract. The cleavage products were analyzed in a urea-containing polyacrylamide gel. For this analysis, a 300-bp Bam HI–Xba I fragment containing the $J_{\lambda}1$ (*3*) sequence was labeled at the Xba I end, and the end-labeled DNA was incubated with the mouse fetal liver nuclear extract (Fig. 2). The reacted DNA was then analyzed on a 6 percent DNA sequencing gel along with a size marker (G reacted $J_{\lambda}1$ DNA). A strong cleavage site was detected between the conserved heptamer and the $J_{\lambda}1$ coding sequence. The faint bands that were present were due to a nonprotein mediated reaction. Prolonged incubation revealed lighter bands adjacent to the main cleavage band; these may be caused by contaminating exonucleolytic activities.

Of the various column resins used to eliminate the DNA degrading activities from the extract, heparin agarose (Bio-Rad) gave the best preparation after the DE52 column. The activity was detected in the 100 m*M* KCl eluate from the heparin agarose column, but not in the 500 m*M* eluate (Fig. 3). Many secondary cleavages were detected both with the 100 m*M* and 500 m*M* eluates. To test the possibility that the

faint cleavages might be due to the chemical nicking of DNA, we incubated the extract at 65°C for 10 minutes before the reaction began, or treated it with proteinase K. The secondary cleavages were not inactivated by proteinase K or by heat treatment. In contrast, the main cleavage activity is both heat labile and sensitive to proteinase K (Fig. 3). These observations indicate that the specific cleavage occurring at the 5′ end of the $J_{\lambda 1}$ gene segment is mediated by a protein, while the secondary cleavages are probably due to a chemical nicking. This is supported by the fact that the reaction buffer alone can generate these nicks. A similar nicking was also observed with a sequencing gel assay to study a rec BC cleavage activity in *Escherichia coli* (*15*). A reaction buffer control was then always used in the cleavage assay to distinguish enzymatic cleavages from chemical cleavages.

This sequencing gel assay only detects the cleavage on one of the two DNA strands. In order to characterize the cleavage on the sense and anti-sense strands at the same time, the $J_{\lambda 1}$ fragment was labeled at the Xba I end either with polynucleotide kinase or the Klenow fragment of DNA polymerase. Both the sense (3′ labeled) and anti-sense (5′ labeled) fragments were reacted with the cleavage extract and separated on a sequencing gel, with chemically reacted portions as markers. The cleavage site consists of a 3′ overhanging guanidine nucleotide ($^{TG}_{A}$) generated at the dinucleotide pair $^{TG}_{AC}$ (Fig. 4). The same results were obtained when a similar experiment was done by labeling the $J_{\lambda 1}$ fragment at the Bam HI end.

Using the $J_{\lambda 1}$ DNA as a substrate, we examined the cleavage activity in different types of cells and tissues (*16*). The myeloma line MPC11 (*17*) was tested for $J_{\lambda 1}$ cleaving activity. Although chemical cleavages were detected, no specific cleavage in the $J_{\lambda 1}$ DNA was observed. A similar result was obtained with the lymphomas 231R (*18*) and K46*R* (*19*). The activity was not present in mouse L cells; it was present in adult mouse liver cells, but not in spleen, brain, and kidney nuclear extracts. The activity in the extract was relatively stable at 0°C, although it could be easily inactivated by treatment at 65°C for 30 seconds. The cleavage was inhibited by high concentrations of salt (300 m*M* Na^+) or deoxynucleotides (100 μ*M*)(or both) (*16*).

In birds, B cell differentiation takes place in the bursa of Fabricius (*11*). To test whether the bursa cells contain a similar endonuclease, we prepared nuclear extract from the bursas of 12- and 14-day-old chick embryos. Chicken Ig genes also contain the conserved heptamer and nonamer sequences at the recombination site (*20*). Using mouse Ig DNA as a substrate, we tested the bursa cell extract for cleavage activity. Three strong cleavages are detected in the D region with both extracts. Although the chicken extract is less contaminated with the exonucleolytic activity, both patterns are basically the same. Similar results were obtained when the cleavage assay was done on the mouse J_κ and J_H gene segments (*20*). The cleavage often occurs at CCA or TGG (Figs. 2 and 5), although not all the CCA or TGG sites are cleaved. Some cleavages take place at the dinucleotide pair $^{TG}_{AC}$ as well (*20*), indicating a probable specificity of this endonuclease for this dinucleotide pair. This suggests that correct cleavage in vivo not only requires a particular primary sequence at the cleavage site but also specific secondary or tertiary structure of the chromatin.

The immunoglobulin genes are activated by somatic DNA recombination. Although the developmentally regulated gene rearrangement has been extensively analyzed, these analyses have revealed little about the molecular mechanisms of Ig gene recombination but have provided sequence informa-

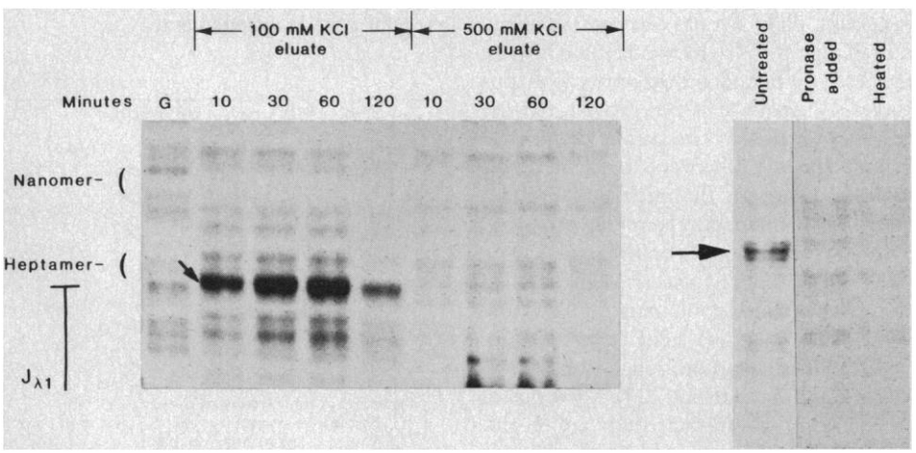

Fig. 3 (above). Partial purification of the endonucleolytic activity. Crude extract of mouse fetal liver nuclei was passed through a DE52 column to remove nonspecific DNA degradation activities. The flow through eluate (−KCl) was then further purified by salt washes of a heparin agarose column. The activity was eluted from the column with 100 m*M* KCl. The specific cleavage is detected in the $J_{\lambda 1}$ DNA with the 100 m*M* eluate, but not with the 500 m*M* eluate (although many faint chemical cleavages occur even with the 500 m*M* eluate). If the extract is treated with proteinase K or heated at 65°C for 5 minutes prior to the cleavage reaction, the specific cleavage reaction does not occur, while the secondary cleavages still take place.

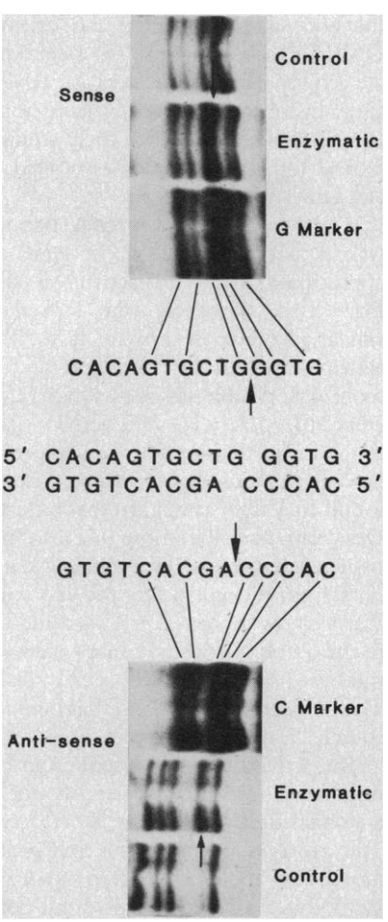

Fig. 4 (right). Characterization of in vitro cleavage site of $J_{\lambda 1}$ gene segment. The $J_{\lambda 1}$ gene segment was labeled at the Xba I end using kinase to label the 5′ overhanging strand and Klenow fragment to label the 3′ end of the other strand. G or C reacted samples were used as size markers. Contaminating exonucleolytic degradation normally causes multiple banding in this assay. To avoid this problem we reacted the end-labeled samples for only 5 minutes in this experiment. The enzymatic cleavage level is almost the same as the chemical cleavage detected in this limited reaction. These results indicate that the cleavage product consists of a 3′ overhanging guanidine nucleotide generated by cleavage at the dinucleotide TG. The same results were obtained when the experiment was repreated by labeling at the Bam HI end.

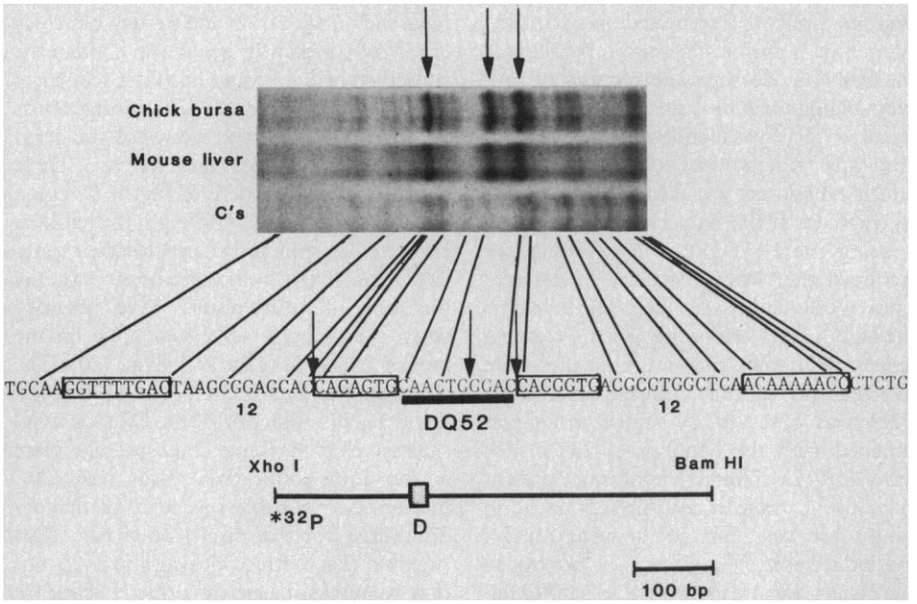

Fig. 5. In vitro cleavage of the Xho I–Bam HI D_{Q52} gene segment with nuclear extracts of mouse fetal liver and chick embryo bursa cells. A Maxam-Gilbert C-reacted sample was separated as a size marker with the cleavage products. The cleavage patterns with the mouse fetal liver and chick embryo bursa nuclear extracts are basically the same.

tion for the DNA around the recombination site. In our studies of Ig gene recombination, we assume that three activities are associated with the putative recombinase; (i) a DNA binding activity that recognizes the two signal sequences and orients the DNA for recombination, (ii) an endonuclease activity that cuts or nicks the DNA, and (iii) a ligase activity that covalently joins the cleaved DNA. To initiate these studies, we looked for a recombinase-associated cleavage activity.

We have identified a specific endonucleolytic activity that cleaves Ig genes at an appropriate site. This activity is distinct from those of others who looked for a similar recombinase activity (*21, 22*). The activity reported by Desiderio and Baltimore cuts double-stranded DNA in $\frac{G}{C}$ rich areas in J_κ DNA (*21*). The activity (*21*) was found in an Abelson transformed pre–B cell line and in mouse L cells. Kataoka *et al.* (*22*) found an activity similar to that reported by Desiderio and Baltimore (*21*) in natural tissues (adult mouse liver and chick embryo bursa) but did not detect the endonuclease that we now report (*22*). This could be due to the 5 m*M* adenosine triphosphate (ATP) they used to inhibit nonspecific nucleases. This concentration of ATP inhibited our specific cleavage completely.

The activity that we describe can be distinguished from the previously identified endonuclease (*21, 22*) by several criteria. The activity that we report is only present in mouse liver and chick embryo bursa, whereas the other one is present in all cells and tissues analyzed. Our activity is inhibited by 100 μ*M* concentrations of any deoxynucleotides whereas the other nuclease can function under conditions of at least 5 m*M* adenosine triphosphate (ATP). These facts along with differences in cleavage specificity indicate that the activity we describe is quite distinct from that identified in two previous studies. Although it is not proved that the cleavages we observe are part of the normal recombination mechanism, this activity is a good candidate for the nuclease associated with the recombination complex.

The in vitro cleavages on the mouse D_{Q52} DNA correspond to the sites at which a transfected plasmid containing the D_{Q52} and J_H (H, heavy chain) gene segments can rearrange in an Abelson transformed pre–B cell line during culturing (*23*). Two out of the four examples in their study are recombined at the site most 3′ shown in Fig. 5, while a third is recombined one nucleotide 5′ of this site. The fourth example is rearranged at the site of the conserved cleavage site located in the D_{Q52} coding region. These data from artificial systems may indicate that there is more than one possible site for the recombination of the D_{Q52} gene segment with the J_H genes.

The endonuclease cuts at the dinucleotide pair $\frac{TG}{AC}$ but it does not cut at all such pairs. Possibly the cleavage activity requires an associated DNA binding activity that provides specificity for TG dinucleotides in the area of a conserved heptamer. The possible importance of the dinucleotide TG in immunoglobulin gene rearrangement was also noted when the frequency of the use of the J_κ gene segments in mouse κ loci rearrangement was analyzed (*24*). The results show that those gene segments with a second TG dinucleotide near the conserved heptamer rearrange at a much higher frequency. A similar correlation can also be seen in the preferential involvement of those gene segments that have a second TG dinucleotide in the murine λ and human κ gene segments. It is also interesting that the dinucleotide pair $\frac{TG}{AC}$ can often be seen at the site of *myc* oncogene translocations (*25, 26*) and heavy chain switch recombinations (*27, 28*), which take place in B lymphocytes.

In our study, a specific endonuclease activity was found in mouse fetal and adult liver cells, as well as chick embryo bursa. Although the activity is expected in mouse fetal liver and chick embryo bursa, the unexpected finding of the activity in adult mouse liver might be due to the presence of contaminating lymphocytic populations. The activity exhibits a specificity for the dinucleotide base pair $\frac{TG}{AC}$. Recent studies of the recombination of retrovirally inserted κ gene segments suggest that a cleavage is taking place just after the dinucleotide $\frac{TG}{AC}$ in the conserved heptamer (*29*). Because the activity that we report has a specificity for $\frac{TG}{AC}$ we suggest that this is a good candidate for the endonuclease involved in immunoglobulin gene rearrangement.

REFERENCES AND NOTES

1. S. Tonegawa, *Nature (London)* **302**, 575 (1983).
2. O. Bernard, N. Hozumi, S. Tonegawa, *Cell* **15**, 1 (1978).
3. H. Sakano, K. Huppi, G. Heinrich, S. Tonegawa, *Nature (London)* **280**, 370 (1979).
4. J. Seidman, E. Max, P. Leder, *ibid.* **280**, 370 (1979).
5. E. Max, J. Seidman, P. Leder, *Proc. Natl. Acad. Sci. U.S.A.* **76**, 3450 (1979).
6. H. Sakano, R. Maki, Y. Kurosawa, W. Roeder, S. Tonegawa, *Nature (London)* **286**, 676 (1980).
7. P. Early, H. Huang, M. Davis, K. Calame, L. Hood, *Cell* **19**, 981 (1980).
8. H. Sakano, Y. Kurosawa, M. Weigert, S. Tonegawa, *Nature (London)* **290**, 562 (1981).
9. H. Sakano, in *Immunology '83*, T. Tada *et al.*, Eds. (Nakayama, Tokyo, 1983), p. 1389.
10. J. Owen, M. Cooper, M. Raff, *Nature (London)* **249**, 361 (1974).
11. B. Glick, T. Chang, R. Jaap, *Poultry Sci.* **35**, 224 (1956).
12. J. Dignam, R. Lebowitz, R. Roeder, *Nucleic Acids Res.* **11**, 1475 (1983).
13. A. Maxam and W. Gilbert, *Methods Enzymol.* **65**, 498 (1980).
14. E. Southern, *J. Mol. Biol.* **98**, 503 (1975).
15. A. Talor, D. Schultz, A. Ponticelli, G. Smith, *Cell* **41**, 153 (1985).
16. T. Hope, R. Aguilera, H. Sakano, in preparation.
17. Y. McHugh, M. Yagi, M. Koshland, in *B-Lymphocytes in the Immune Response*, N. Klinman *et al.*, Eds. (Elsevier, New York, 1981), p. 467.
18. R. Zinkernagel *et al.*, *J. Exp. Med.* **147**, 882 (1978).
19. K. Kim, C. Kanellopoulos-langevin, G. Chaouat, R. Asofsky, *B-Lymphocytes in the Immune Response*, N. Klinman *et al.*, Eds. (Elsevier, New York, 1981), p. 507.
20. C. Reynaud, V. Anquez, A. Dahan, J. Weill, *Cell* **40**, 283 (1985).
21. S. Desiderio and D. Baltimore, *Nature (London)* **308**, 860 (1984).

22. T. Kataoka, S. Kondo, M. Nishi, M. Kodaira, T. Honjo, *Nucleic Acids Res.* 12, 5995 (1984).
23. T. Blackwell and F. Alt, *Cell* 37, 105 (1984).
24. D. Wood and C. Colecough, *Proc. Nat. Acad. Sci. U.S.A.* 81, 4756 (1984).
25. S. Gerondakis, S. Cory, J. Adams, *Cell* 36, 973 (1984).
26. L. Corcoran, S. Cory, J. Adams, *ibid.* 40, 71 (1985).
27. T. Nikaido, Y. Yamawaki-Kataoka, T. Honjo, *J. Biol. Chem.* 257, 7322 (1982).
28. R. Aguilera, T. Hope, H. Sakano, *EMBO J.* 4, 3689 (1985).
29. S. Lewis, A. Gifford, D. Baltimore, *Science* 228, 677 (1985).
30. Supported by NIH grant AI-18790, and ACS grant IM-366 and a predoctoral fellowship from NSF (R.J.A.). We thank Dr. Anthony Otsuka for critical reading of the manuscript and Dr. Olli Vainio for advice on the preparation of chick embryo bursa.

7 June 1985; accepted 5 December 1985

Atrial Natriuretic Peptide Elevation in Congestive Heart Failure in the Human

J. C. BURNETT, JR.,* P. C. KAO, D. C. HU, D. W. HESER, D. HEUBLEIN, J. P. GRANGER, T. J. OPGENORTH, G. S. REEDER

A sensitive radioimmunoassay for atrial natriuretic peptide was used to examine the relation between circulating atrial natriuretic peptide and cardiac filling pressure in normal human subjects, in patients with cardiovascular disease and normal cardiac filling pressure, and in patients with cardiovascular disease and elevated cardiac filling pressure with and without congestive heart failure. The present studies establish a normal range for atrial natriuretic peptide in normal human subjects. These studies also establish that elevated cardiac filling pressure is associated with increased circulating concentrations of atrial natriuretic peptide and that congestive heart failure is not characterized by a deficiency in atrial natriuretic peptide, but with its elevation.

RECENT INVESTIGATIONS HAVE documented the existence of specific secretory granules that have vasoactive properties (*1–6*). Studies from various laboratories have established that administration of synthetic atrial natriuretic peptide (ANP) in animals results in natriuresis, decrease in arterial pressure, and inhibition of the renin-angiotensin-aldosterone system, supporting a role for the atrial peptide system in cardiovascular volume regulation (*7, 8*). Thrasher and colleagues have reported that acute increases in cardiac filling pressures in conscious dogs result in enhanced release of circulating ANP, suggesting that cardiac volume or pressure or both may be important in determining the release of ANP (*9*). Chimoskey and co-workers have reported that hamsters with familial cardiomyopathy and congestive heart failure are deficient in ANP as determined by bioassay (*10*). These investigators speculated that failure to produce sufficient ANP by the degenerating hearts of cardiomyopathic hamsters contributes to the retention of sodium and water with formation of edema. No studies have been performed to define the relation in humans between circulating levels of ANP and cardiac filling pressures. Further, no studies have established whether the syndrome of congestive heart failure is characterized by a deficiency in ANP.

We determined circulating concentrations of ANP in normal human volunteers with no history of cardiovascular disease (group 1, n = 14), patients with cardiovascular disease but normal cardiac filling pressures (group 2, n = 11), patients with cardiovascular disease and markedly elevated cardiac filling pressures but without congestive heart failure (group 3, n = 6), and patients with cardiovascular disease, markedly elevated cardiac filling pressures, and congestive heart failure (group 4, n = 6).

We determined the circulating concentrations of ANP with a newly developed, sensitive, nonequilibrium radioimmunoassay for human α-ANP. The synthetic peptide of human α-ANP (Peninsula Laboratory) was used to prepare standard and tracer. We labeled human α-ANP with $Na^{125}I$ by the Iodogen procedure. The crude, labeled peptide was purified first on a Bio-Rad P-2 column and then by high-performance liquid chromatography (HPLC) on a C_{18} column (Fig. 1A). For the radioimmunoassay, we first incubated rabbit antiserum to human α-ANP (RAS-8798, Peninsula Laboratory) in the presence of standard or sample for 24 hours and then added the labeled ANP for an additional 16 hours of incubation, both at 4°C. Free and bound fractions

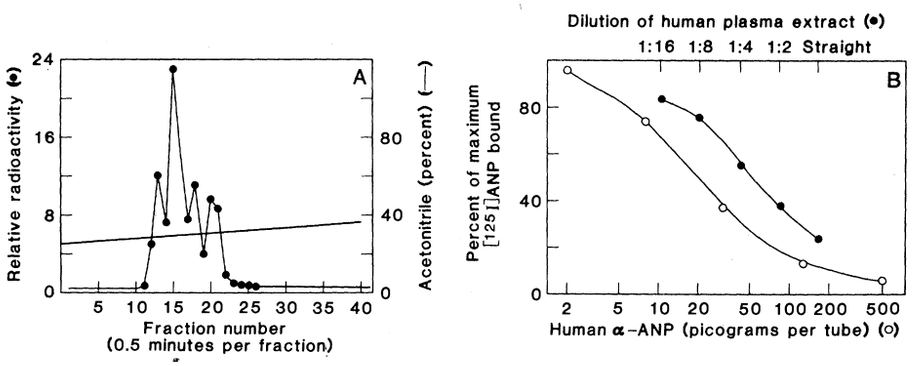

Fig. 1. Radioimmunoassay for human α-ANP. Synthetic human α-ANP (2 μg in 20 μl of 0.5*M* sodium phosphate buffer, *p*H 7.4) was iodinated with 2 mCi of $Na^{125}I$ (Amersham) by 2.5 μg of Iodogen (Pierce Chemical), which had been dissolved in dichloromethane and evaporated to dryness in a test tube. The reaction mixture was first purified on a Bio-Rad P-2 column (0.8 by 15 cm) eluted with 0.1*M* acetic acid containing 0.1 percent bovine serum albumin (BSA). Then it was further purified on a μBondapak C_{18} column with a linear gradient of 25 to 35 percent acetonitrite in a solution of 0.1 percent trifluoroacetic acid. Four peaks showing radioactivity were obtained (A), all of which had equivalent immunobinding ability with rabbit antiserum to human α-ANP. The second peak was used for the radioimmunoassay. The purified, labeled human α-ANP was diluted in assay buffer (0.1*M* sodium phosphate, 0.05*M* NaCl, 0.1 percent BSA, 0.1 percent Triton X-100, and 0.01 percent sodium azide) to a concentration of 10,000 counts per minute per 100 μl as total count per tube. Rabbit antiserum to human α-ANP was also diluted in assay buffer to a concentration such that 100 μl of the solution would bind 35 percent of the total count in the absence of standard. The standard curve was constructed by serial dilution of synthetic human α-ANP from 500 pg to 1.8 pg per 100 μl. The antibody and standard were incubated together for 24 hours at 4°C, after which labeled human α-ANP was added to incubate for an additional 16 hours, both at 4°C. Free and bound fractions were separated by precipitation with the second antiserum in the presence of 2 percent polyethylene glycol 8000. The mixtures were incubated for 30 minutes at 4°C and then centrifuged. The supernatants, or free fractions, were aspirated and discarded; the precipitates, or bound fractions, were counted in a gamma counter, and standard curves were calculated (open circles in B). A curve constructed from results of a serial dilution of a human plasma extract with assay buffer showed parallelism to the standard curve (closed circles in B).

Departments of Internal Medicine and Laboratory Medicine, Mayo Medical School, Rochester, MN 55905.

*To whom correspondence should be addressed.